Supplementary Materials for

ACE2-Targeting Monoclonal Antibody As A "Pan" Coronavirus Blocker

Yuning Chen[1,7,*], Yanan Zhang[2,7,*], Renhong Yan[3,*], Guifeng Wang[1], Yuanyuan Zhang[3], Zherui Zhang[2,7], Yaning Li[5], Wendi Chu[1], Yili Chen[4], Ganjun Chen[4,7], Qi Wang[1], Qiang Zhou[3]†, Bo Zhang[2,6]†, Chunhe Wang[1,4]†

This PDF file includes:

Materials and Methods

Protein expression and purification

The 6×His-tagged S1 proteins of SARS-CoV-2 D614G, SARS-CoV-2 (D614), SARS-CoV and HCoV-NL63 were purchased from Sino Biological (Beijing, China). ACE2-his, ACE2-Fc and 3E8 were prepared as below: The DNA fragments encoding extracellular ACE2 domain (residues 19-740) from plasmid encoding full-length ACE2 (Sino Biological) was subcloned into the mammalian expression vectors pTT5 and pINFUSE (Invivogen, San Diego, CA) with a C-terminal 6×His and hIgG1-Fc tags, respectively. The codon-optimized variable regions of the heavy and light chain of 3E8 were cloned into expression vectors containing human IgG4 constant regions. Purified plasmids were transfected into HEK293F cells (Shanghai Cell Line Bank, China) by polyethylenimine (Polysciences, Warrington, PA). Cells were then cultured in suspension in OPM-293 CD05 medium (Shanghai OPM BIosciences). After 5 days of culture, the supernatant was collected and purified by Ni-NTA or protein A chromatography. Size exclusion column (SEC)-HPLC was used to measure the purity of proteins.

Biolayer interferometry (BLI)

Binding affinities were measured by BLI using Fortebio Octet Red 96. For affinity measurement, 15 μg/ml of 6×His-tagged human ACE2 protein was captured by Ni-NTA biosensor and incubated with different concentrations of 3E8. For S1-proteins binding to ACE2, 15 μg/ml of 6×His-tagged S1 proteins were immobilized on Ni-NTA

biosensor and incubated with serial dilutions of recombinant ACE2-Fc fusion protein. The baseline was established by PBS with 0.05% Tween-20 for 60 s. Both of the association and the dissociation periods were set at 400 s. The mean Kon, Koff and apparent KD values of binding affinities were calculated from all binding curves based on their global fit to a 1:1.

Binding ELISA

96-well Immuno-plates (Greiner bio-one) were coated with 2.0 μg/ml of purified recombinant 6×His-tagged human ACE2 protein at 4℃ overnight. After blocking at room temperature for 1 h with 1% casein (Thermo Fisher), plates were washed with PBS containing 0.05% Tween-20, and serial dilutions of 3E8 were added for 1 h incubation. After washing, goat anti-human IgG conjugated with HRP (ABclonal Technology, 1:2000 dilution) was added and incubated for 1 h, then TMB substrate (Thermo Fisher Scientific) and 2 M of H_2SO_4 were added, and OD_{450} was detected with SpectraMax M5e (Molecular Devices) microplate reader. To measure the binding affinity of S1 proteins to ACE2, 2 μg/ml of various S1 proteins were coated into plates followed by the addition of gradient diluted ACE2-Fc, and goat anti-human IgG conjugated with HRP was used for detection.

Neutralization ELISA

S1-proteins (2 μg/ml) were coated in plates at 4℃ overnight. Serial dilutions of 3E8 or isotype were pre-incubated with 5 μg/ml of ACE2-Fc for 30 min at room temperature.

Then, the mixture was added into the coated plate wells and incubated for 1h. The bound ACE2-Fc was detected by HRP-conjugated goat anti-human IgG and developing substrate.

Flow Cytometry

Vero E6 and HEK293/ACE2/EGFP cells were harvested and aliquoted into FACS tubes at 5×10^5 cells/tube. The cells were washed with cold staining buffer (PBS+0.1% BSA+0.04% Na3N) and then resuspended in 100 μl of 3E8 at different concentrations. The cells were kept at 4℃in the dark for 1 h on a shaker before washed twice. The cells were resuspended in 100 μl of staining buffer containing PE-goat-anti-human IgG (Biolegend) at 4 μg/ml for 30 min. The cells were washed twice and resuspended in 200 μl of staining buffer for flow cytometry analysis.

Western Blot

Vero E6 cells were incubated at 37℃ with different concentrations of 3E8 in DMEM with 10% FBS and lysed with commercial cell lysis buffer (Beyotime, Shanghai, China) at different time points. Western blot analysis for ACE2 protein in whole cell lysate was carried out using rabbit anti-ACE2 pAb (1:500, Sino biological) and goat anti-rabbit conjugated with HRP (1:2000, Abclonal, Wuhan, China) using a standard Western blot protocol.

Live virus neutralization assay

Vero E6 (ATCC® CRL-1586™) cells were trypsinized and pre-seeded into 24-well plates in duplicate with 1×10^5 cells/well in DMEM containing 10% FBS (100 U/mL of penicillin and 100 μg/ml of streptomycin) at 37℃with 5% CO_2 one day before. After confluent, antibodies of 3-fold serially diluted were added, and Vero E6 cells were infected with live SARS-CoV-2 (IVCAS 6.7512) virus at a multiplicity of infection (MOI) of 0.01. After 24h incubation, the culture supernatants were collected and viral RNA were quantified via qRT-PCR using Luna® Universal Probe One-Step RT-PCR Kit (E3006) on CFX96 Touch^{TM} Real-Time PCR Detection System (Bio Rad). Primers used were as follows: RBD-qF1: 5'-caatggtttaacaggcacagg-3', RBD-qR1: 5'-ctcaagtgtctgtggatcacg-3', Probe: acagcatcagtagtgtcagcaatgtctc. IC_{50} was fitted and calculated by GraphPad Prism 8. Data represents as mean ± SD of two replicates from one representative experiment, and the experiment was repeated for 3 times.

Pseudo-typed virus neutralization assay

Pseudo-typed SARS-CoV-2-D614G, SARS-CoV-2, SARS-CoV and HCoV-NL63 were constructed by co-transfection of two plasmids, one expressing Env-defective HIV-1 with luciferase reporter (pNL4-3.luc.RE)(*1*) and the other expressing the full-length S-protein of SARS-CoV-2-D614G, SARS-CoV-2, SARS-CoV or HCoV-NL63, into HEK293T cells. The supernatant containing virus particles was harvested 48 h post-transfection followed by 0.45 μm filtration.

HEK293F/ACE2/EGFP cells were pre-seeded with 1.2×10^4 cells per well in a 96-well plate. The confluent cells were incubated with 50 μl of serially-diluted antibodies

or ACE2-Fc for 1h at 37℃ followed by addition of various pseudoviruses of the same volume. 100 μl of DMEM with 10% FBS was added as negative control. 100 μl of pseudovirus and DMEM mixed at ratio 1:1 was used as positive control. After 24 h, medium was change and the cell incubated for another 48 h. The relative light units (RLUs) of luminescence was measured by Firefly Luciferase Reporter Assay Kit (Meilunbio). Neutralization (%) = [1- ($RFU_{samples}$ - $RFU_{negtive\ control}$) / ($RFU_{positive\ control}$ - $RFU_{negtive\ control}$)] ×100%. The IC_{50} values were calculated by non-linear regression in GraphPad Prism 8.

Animal study for live virus neutralization

BALB/c mice were purchased from Wuhan Institute of Biological Products Co. Ltd. and cared in accordance with the recommendations of National Institutes of Health Guidelines for the Care and Use of Experimental Animals. All the animal studies were conducted in biosafety level 3 (BSL-3) facility at Wuhan Institute of Virology under a protocol approved by the Laboratory Animal Ethics Committee of Wuhan Institute of Virology, Chinese Academy of Sciences (Permit number: WIVA26201701).

A mouse model recently established by VEEV-VRP delivery of ACE2 for SARS-CoV-2 infection (*2*) was used to evaluate the efficacy of 3E8 in vivo. Four groups of six- to eight-week-old female BALB/c mice (n=5 per group) were first intranasally infected with 10^6 FFU VRP-ACE2 per mouse in a total volume of 80 μl after anesthetization with Avertin (250 mg/kg). 12h later, the mice from different groups were treated with 3E8, B38 or isotype at a dose of 10 mg/kg via intraperitoneal injection, respectively.

After another 12 h, all mice were intranasally infected with 10^5 PFU SARS-CoV-2 in a total volume of 50 μl. 3 days post infection of SARS-CoV-2, the lungs of mice were collected for viral RNA quantification and histological analysis. For RNA quantification, some lungs were homogenized in DMEM medium, and viral RNA was extracted using QIAamp viral RNA mini kit （52906, Qiagen） following the manufacturer's protocol. qRT-PCR assay was performed using Luna® Universal Probe One-Step RT-PCR Kit (E3006). Primers and probe used were: RBD-qF1: 5'-caatggtttaacaggcacagg-3', RBD-qR1: 5'- ctcaagtgtctgtggatcacg -3', Probe: acagcatcagtagtgtcagcaatgtctc. For histological analysis, lung samples from mice were fixed with 4% paraformaldehyde, embedded in paraffin, sagittally sectioned at 4 μm thickness on a microtome, and mounted on APS-coated slides for H&E stain.

ACE2 enzymatic activity assays

The catalytic activities of recombinant and endogenous ACE2 was detected according to a published protocol using fluorescent substrate, Mca-APK-Dnp (AnaSpec) (*3*). To determine the impact on enzyme activity, serial diluted antibodies were pre-incubated with 2.0 μg/ml of recombinant human ACE2 at room temperature for 1 h on a shaker. After incubation, the neutralization solution was 1:5 diluted with activity buffer (*3*) and then mixed with 50 μl/well of 200 mM substrate. The mixture was incubated at 37 °C for 20 min before the RFU of fluorescent signals were read on an Envision microplate reader (Perkin Elmer, Waltham, MA) with excitation wavelength set at 320 nm and emission wavelength set at 400 nm. To measure endogenous ACE2 enzymatic activity,

Vero E6 cells were seeded in a 96-well plate at 1×10^5 cells/well and cultured overnight. The cells were then incubated with 10 μg/ml of 3E8, AF933(R&D Systems, Minneapolis, MN) and isotype for 60 min at 37℃ before mixed with 50 μl/well of activity buffer and 50 μl/well of substrate. The cells were incubated for 20 min at 37℃ before transferred to black 96-well plate for fluorescence reading.

Cryo-EM sample preparation

The ACE2-B^0AT1 complex was mixed with 3E8 at a molar ratio of 1:1.5 at 4 °C for 1hr before applied to the grids. Aliquots (3.3 μl) of the protein complex were placed on glow-discharged holey carbon grids (Quantifoil Au R1.2/1.3). The grids were blotted for 2.5 s or 3.0 s and flash-frozen in liquid ethane cooled by liquid nitrogen with Vitrobot (Mark IV, Thermo Scientific). The cryo-EM samples were transferred to a Titan Krios operating at 300 kV equipped with Cs corrector, Gatan K3 Summit detector and GIF Quantum energy filter. Movie stacks were automatically collected using AutoEMation (*4*), with a slit width of 20 eV on the energy filter and a defocus range from -1.2 μm to -2.2 μm in super-resolution mode at a nominal magnification of 81,000×. Each stack was exposed for 2.56 s with an exposure time of 0.08 s per frame, resulting in a total of 32 frames per stack. The total dose rate was approximately 50 e^- /$Å^2$ for each stack. The stacks were motion corrected with MotionCor2 (*5*) and binned 2-fold, resulting in a pixel size of 1.087 Å/pixel. Meanwhile, dose weighting was performed (*6*). The defocus values were estimated with Gctf (*7*).

Cryo-EM data processing

Particles were automatically picked using Relion 3.0.6 (*8-11*) from manually selected micrographs. After 2D classification with Relion, good particles were selected and subject to two cycle of heterogeneous refinement without symmetry using cryoSPARC (*12*).The good particles were selected and subjected to Non-uniform Refinement (beta) with C1 symmetry, resulting in the 3D reconstruction for the whole structures, which was further subject to 3D classification, 3D auto-refinement and post-processing with Relion with C2 symmetry. To further improve the map quality for interface between 3E8 and ACE2-B^0AT1 complex, the particles were C2-symmetry expanded and re-centered at the location of the interface between 3E8-ACE2 sub-complex. The re-extracted dataset was subject to focused refinement with Relion, resulting in the 3D reconstruction of better quality on the binding interface.

The resolution was estimated with the gold-standard Fourier shell correlation 0.143 criterion (*13*) with high-resolution noise substitution (*14*). Refer to Supplemental Figures S4-S6 and Supplemental Table S1 for details of data collection and processing.

Cryo-EM model building and structure refinement

For model building of 3E8 bound with ACE2-B^0AT1 complex, the atomic model of the published structure S-ECD (PDB ID: 7C2L) and ACE2-B^0AT1 complex (PDB ID: 6M18) were used as templates, which were molecular dynamics flexible fitted (MDFF) (*15*) into the whole cryo-EM map of the complex and the focused-refined cryo-EM map of the 3E8-ACE2 sub-complex, respectively. And the fitted atomic models were further

manually adjusted with Coot (*16*). Each residue was manually checked with the chemical properties taken into consideration during model building. Several segments, whose corresponding densities were invisible, were not modeled. Structural refinement was performed in Phenix (*17*) with secondary structure and geometry restraints to prevent overfitting. To monitor the potential overfitting, the model was refined against one of the two independent half maps from the gold-standard 3D refinement approach. Then, the refined model was tested against the other map. Statistics associated with data collection, 3D reconstruction and model building were summarized in Table S1.

Toxicity studies

Five-week-old male human ACE2 "knock-in" mice on C57BL/6 background were purchased from Shanghai Model Organisms Center (Shanghai). Animal handling and procedures were approved and performed according to the requirements of the Institutional Animal Care and Use Committee (IACUC) of Shanghai Institute of Materia Medica. Five male mice were randomized into two groups: 3E8 (3 mice, 9#, 66# and 86#) and isotype (2 mice, 68# and 39#). The mice received an intravenous (i.v.) injection of 100 μl (30 mg/kg) of 3E8 or isotype. The mice were weighed and assessed for behavioral changes at 0, 24, 72 and 144 h time points after injection. Toxicities was evaluated by body weight measuring, serum biochemistry and pathology studies. After 7 days of treatment, all mice were sacrificed by cervical dislocation. Blood, hearts, livers, spleens, lungs and kidneys were collected for biochemistry and pathology studies. Organs were fixed with 10% buffered formalin and subjected to paraffin

embedding before sectioned, deparaffined, rehydrated and stained with Hematoxylin and Eosin (H&E) staining.

Statistical analysis

Data were shown as mean ± SEM or SD. Statistical difference were calculated by Student's t-test, with *$P < 0.05$ considered significant and $P < 0.01$ highly significant.

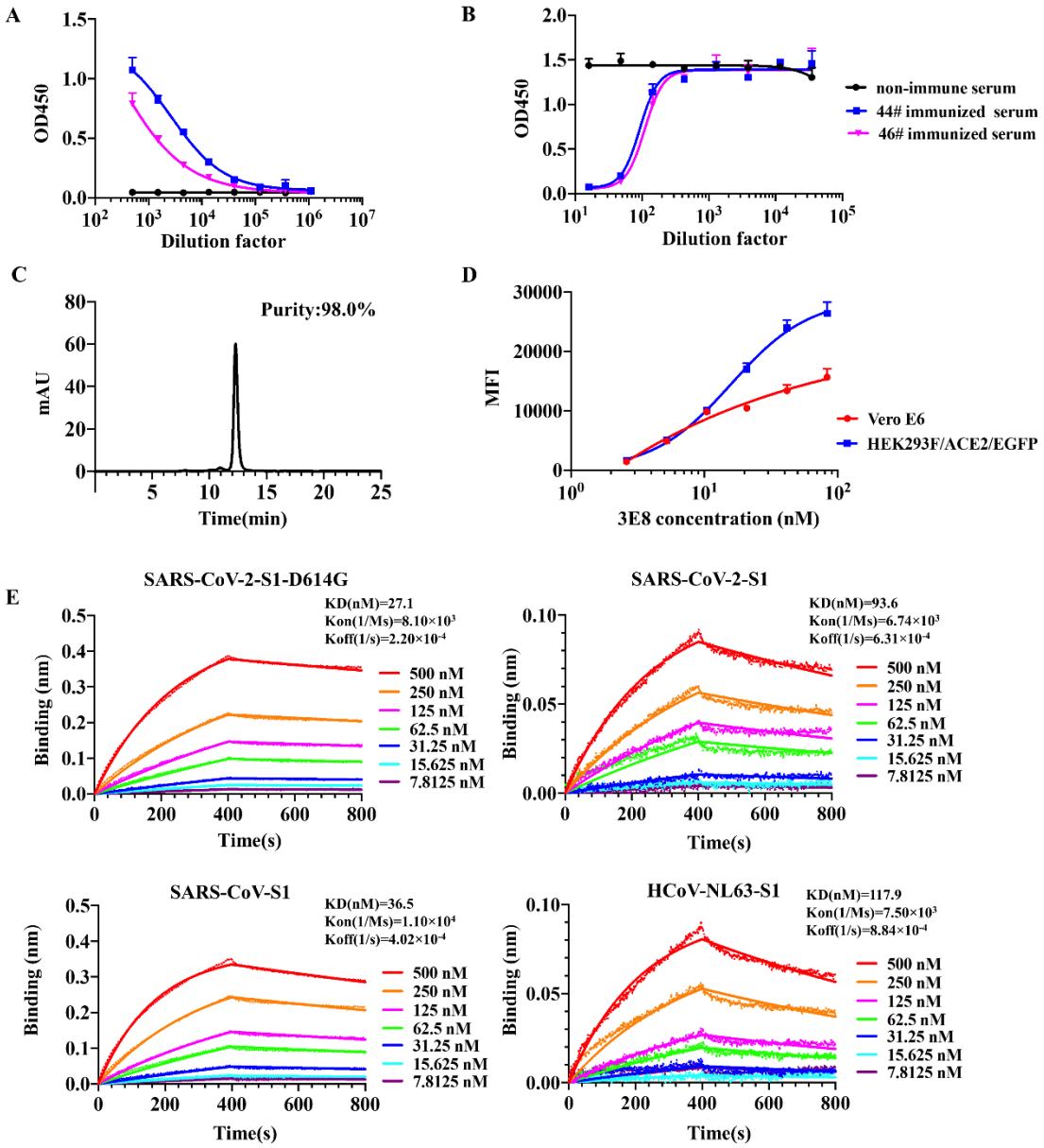

Fig. S1. Bindings of immunized mouse sera and purified monoclonal antibody 3E8 to recombinant human ACE2 protein. Serial dilutions of immunized mouse sera and purified 3E8 were analyzed for binding and neutralization to recombinant human ACE2 protein. (A) Sera from ACE2-immunized mouse bound to His-tagged recombinant human ACE2 protein. (B) Sera from ACE2-immunized mouse neutralized binding of SARS-CoV-2 S1-subunit to His-tagged recombinant ACE2 protein. (C) Purity of 3E8 antibody preparation measured by protein A chromatography. (D) Flow cytometry

analysis of the bindings of S1-subunits from different coronaviruses to HEK293 cells overexpressing human ACE2. (E) The binding affinities of different S1-subunits to human ACE2 recombinant protein as measured by BLI.

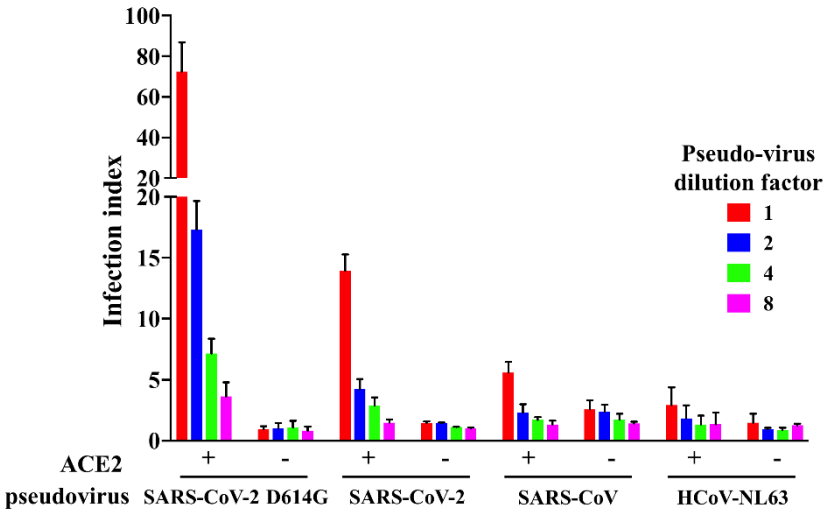

Fig. S2. Infection of HEK293F/ACE2/EGFP cells by different pseudo-typed coronaviruses. Pseudo-typed SARS-CoV-2-D614G, SARS-CoV-2 (D614), SARS-CoV and HCoV-NL63 were constructed and infected HEK293 cells overexpressing human ACE2 and EGFP fusion protein.

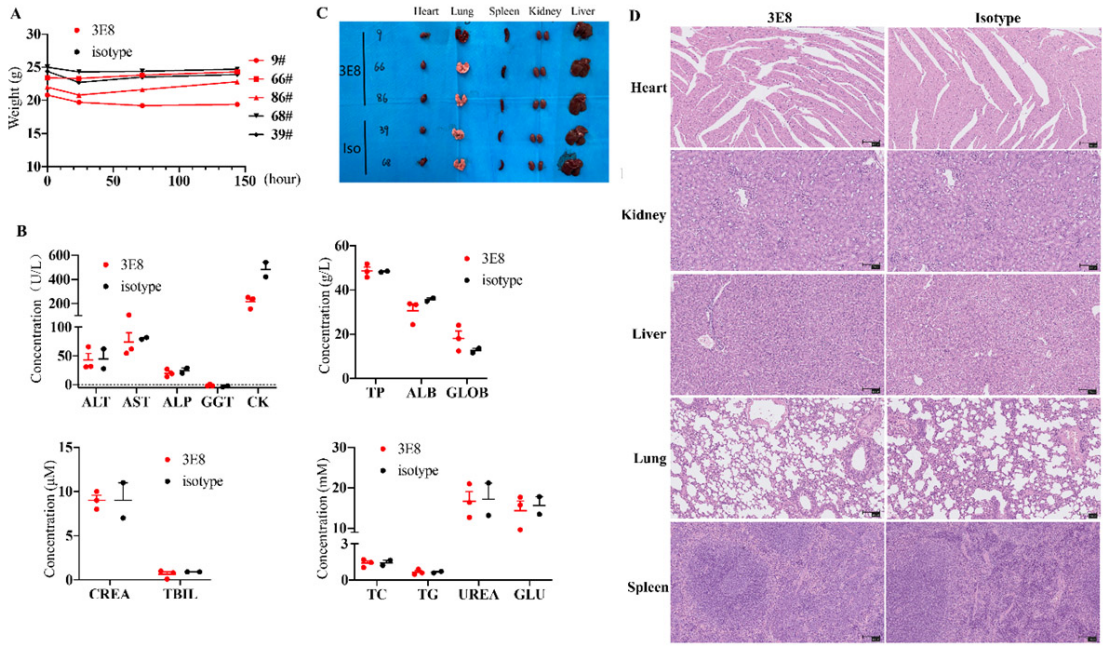

Fig. S3. Toxicity studies of antibody 3E8 in human ACE2 "knock-in" mice. (A) The body weights of the treated mice were measured at 0, 24, 72 and 144 h time points. (B) Blood biochemistry analysis showed the plasma concentrations of alanine transaminase (ALT), aspartate transaminase (AST), alkaline phosphatase (ALP), gamma-glutamyl transpeptidase (GGT), creatine kinase (CK), total protein (TP), albumin (ALB), globulin (GLOB), creatinine (CREA), total bilirubin (TBIL), total cholesterol (TC), triglycerides (TG), urea nitrogen (UREA) and glucose (GLU). The indices of GGT and TBIL in 3E8 group and isotype group were below the normal range, but lowered levels are not signs of toxicity. (C) Shapes and sizes of major organs including hearts, livers, kidneys, spleens and lungs from mice 7 days post treatment. The organs were dissected out after the mice were sacrificed by cervical dislocation and then washed with PBS to clean out the blood. Blood clogging occurred in the lung of mouse 9# during the dissection process, which was determined technical. The mice were otherwise normal.

(D) H&E staining of hearts, livers, kidneys, spleens and lungs of treated mice. No obvious pathological changes were observed. The scale of ratio above represents 100 μm.

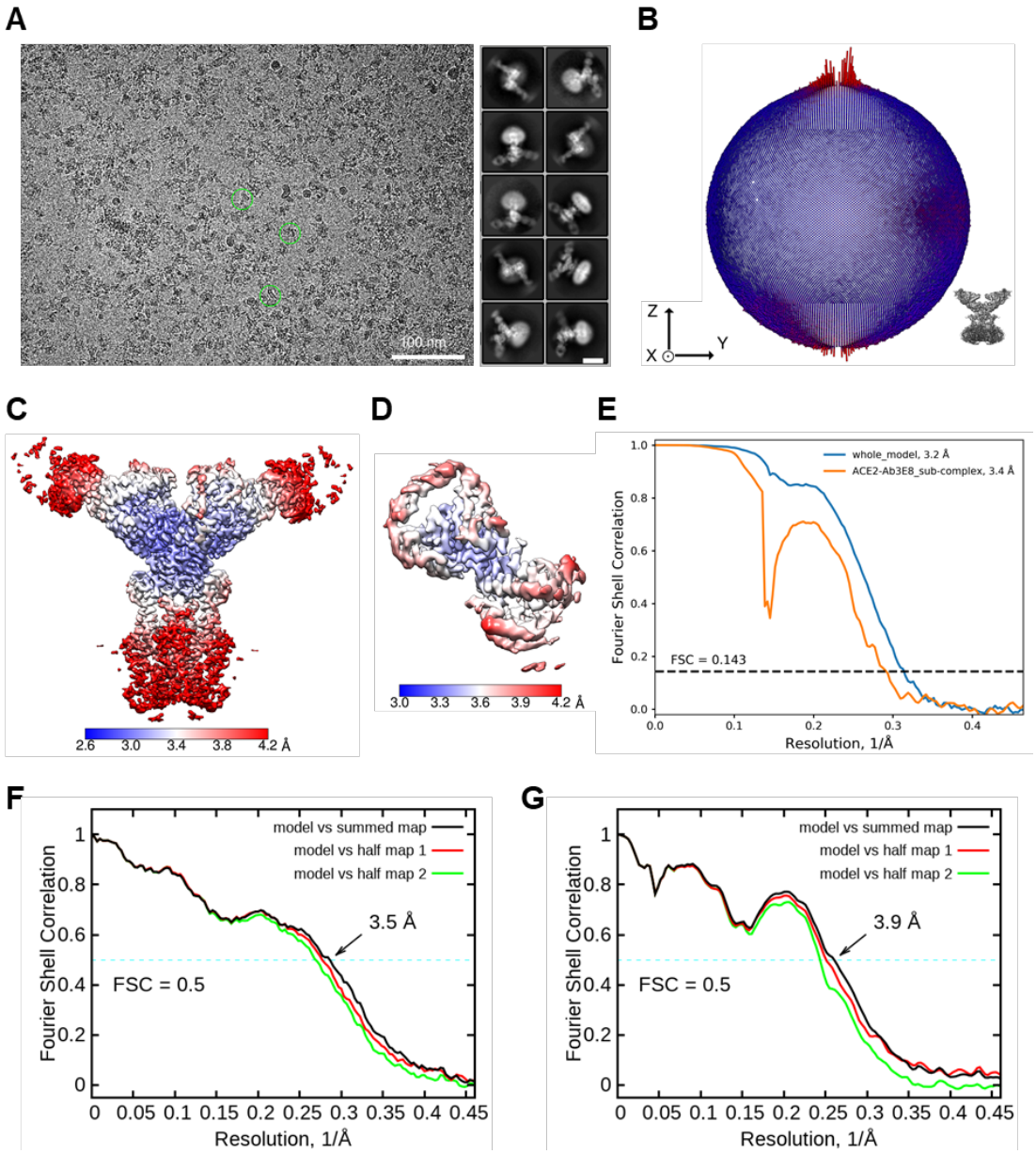

Fig. S4 Cryo-EM analysis of 3E8 bound with ACE2-B^{0}AT1 complex. (A) Representative cryo-EM micrograph and 2D class averages of cryo-EM particle images. The scale bar in 2D class averages is 10 nm. (B) Euler angle distribution in the final 3D reconstruction of 3E8 bound with ACE2-B^{0}AT1 complex. (C) and (D) Local resolution

maps for the 3D reconstruction of overall structure and the 3E8-ACE2 sub-complex, respectively. (E) FSC curve of the overall structure (blue) and 3E8-ACE2 sub-complex (orange). (F) FSC curve of the refined model of 3E8 bound with ACE2-B^0AT1 complex versus the overall structure that it is refined against (black); of the model refined against the first half map versus the same map (red); and of the model refined against the first half map versus the second half map (green). The small difference between the red and green curves indicates that the refinement of the atomic coordinates is not enough overfitting. (G) FSC curve of the refined model of the 3E8-ACE2 sub-complex, which is the same as the (F).

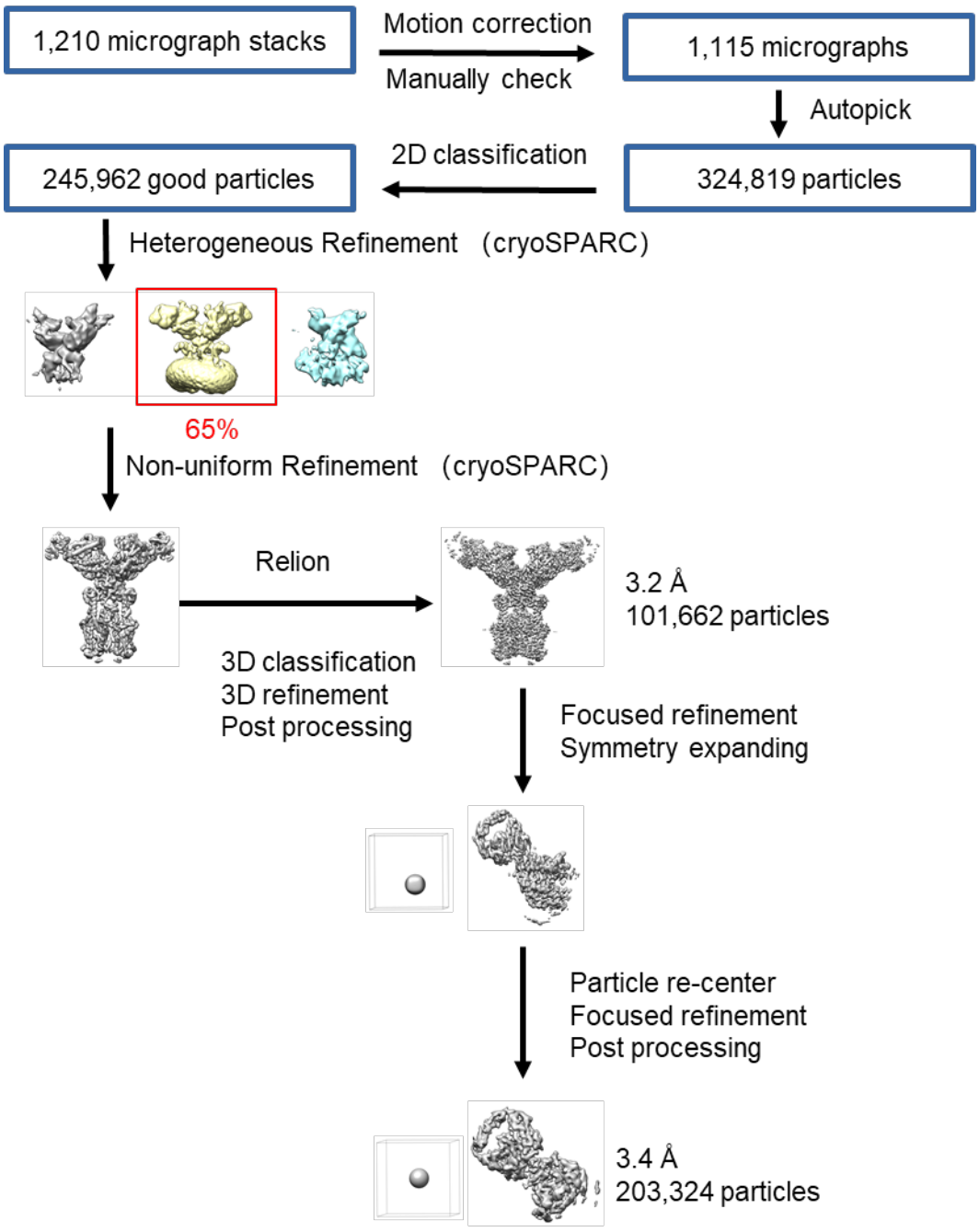

Fig. S5 Flowchart for cryo-EM data processing. Please refer to the 'Data Processing' section in Methods for details.

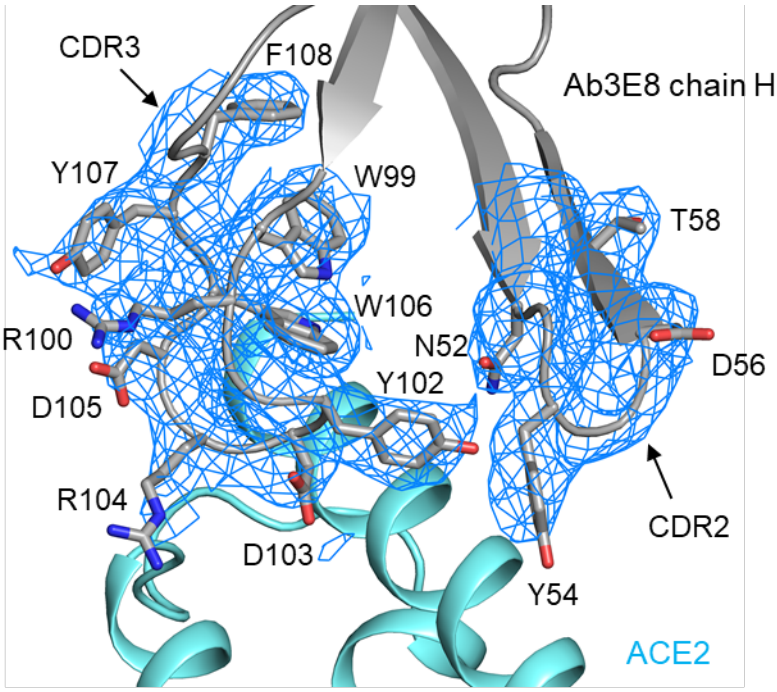

Fig. S6 Representative cryo-EM map densities. Cryo-EM density of the interface between ACE2 and chain H of 4A8. The density is contoured at 10 σ.

Table S1. Cryo-EM data collection and refinement statistics.

Data collection		
EM equipment	Titan Krios (Thermo Fisher Scientific)	
Voltage (kV)	300	
Detector	Gatan K3 Summit	
Energy filter	Gatan GIF Quantum, 20 eV slit	
Pixel size (Å)	1.077	
Electron dose (e-/Å2)	50	
Defocus range (μm)	-1.2 ~ -2.2	
Number of collected micrographs	1,210	
Number of selected micrographs	1,115	
Sample	3E8 bound with ACE2-B0AT1 complex	
3D Reconstruction		
	Whole model	Interface between 3E8 and ACE2
Software	cryoSPARC/ Relion	Relion

Number of used particles	101,662	203,324
Resolution (Å)	3.2	3.4
Symmetry	C2	C1
Map sharpening B factor ($Å^2$)	-90	
Refinement		
Software	Phenix	
Cell dimensions (Å)	310.176	
Model composition		
Protein residues	3,586	
Side chains assigned	3,586	
Sugar	38	
Water	4	
Zn	2	
R.m.s deviations		
Bonds length (Å)	0.010	
Bonds Angle (°)	1.027	
Ramachandran plot statistics (%)		
Preferred	91.53	
Allowed	8.22	
Outlier	0.25	

References and Notes

1. S. Xia *et al.*, Inhibition of SARS-CoV-2 (previously 2019-nCoV) infection by a highly potent pan-coronavirus fusion inhibitor targeting its spike protein that harbors a high capacity to mediate membrane fusion. *Cell Res* **30**, 343-355 (2020).
2. Y. N. Zhang *et al.*, A mouse model for SARS-CoV-2 infection by exogenous delivery of hACE2 using alphavirus replicon particles. **30**, 1046-1048 (2020).
3. K. Liao, D. Sikkema, C. Wang, T. N. Lee, Development of an enzymatic assay for the detection of neutralizing antibodies against therapeutic angiotensin-converting enzyme 2 (ACE2). *J Immunol Methods* **389**, 52-60 (2013).
4. J. Lei, J. Frank, Automated acquisition of cryo-electron micrographs for single particle reconstruction on an FEI Tecnai electron microscope. *J Struct Biol* **150**, 69-80 (2005).
5. S. Q. Zheng *et al.*, MotionCor2: anisotropic correction of beam-induced motion for improved cryo-electron microscopy. *Nat Methods* **14**, 331-332 (2017).
6. T. Grant, N. Grigorieff, Measuring the optimal exposure for single particle cryo-EM using a 2.6 Å reconstruction of rotavirus VP6. *Elife* **4**, e06980 (2015).
7. K. Zhang, Gctf: Real-time CTF determination and correction. *J Struct Biol* **193**, 1-12 (2016).
8. J. Zivanov *et al.*, New tools for automated high-resolution cryo-EM structure determination in RELION-3. *Elife* **7**, (2018).
9. D. Kimanius, B. O. Forsberg, S. H. Scheres, E. Lindahl, Accelerated cryo-EM structure determination with parallelisation using GPUs in RELION-2. *Elife* **5**, (2016).
10. S. H. Scheres, RELION: implementation of a Bayesian approach to cryo-EM structure determination. *J Struct Biol* **180**, 519-530 (2012).
11. S. H. Scheres, A Bayesian view on cryo-EM structure determination. *J Mol Biol* **415**, 406-418 (2012).
12. A. Punjani, J. L. Rubinstein, D. J. Fleet, M. A. Brubaker, cryoSPARC: algorithms for rapid unsupervised cryo-EM structure determination. *Nat Methods* **14**, 290-296 (2017).
13. P. B. Rosenthal, R. Henderson, Optimal determination of particle orientation, absolute hand, and contrast loss in single-particle electron cryomicroscopy. *J Mol Biol* **333**, 721-745 (2003).
14. S. Chen *et al.*, High-resolution noise substitution to measure overfitting and validate resolution in 3D structure determination by single particle electron cryomicroscopy. *Ultramicroscopy* **135**, 24-35 (2013).
15. L. G. Trabuco, E. Villa, K. Mitra, J. Frank, K. Schulten, Flexible fitting of atomic structures into electron microscopy maps using molecular dynamics. *Structure* **16**, 673-683 (2008).

16. P. Emsley, B. Lohkamp, W. G. Scott, K. Cowtan, Features and development of Coot. *Acta Crystallogr D Biol Crystallogr* **66**, 486-501 (2010).
17. P. D. Adams *et al.*, PHENIX: a comprehensive Python-based system for macromolecular structure solution. *Acta Crystallogr D Biol Crystallogr* **66**, 213-221 (2010).